Energization of relativistic electrons in the presence of ULF power and MeV microbursts: Evidence for dual ULF and VLF acceleration

T. P. O'Brien,[1] K. R. Lorentzen,[1,2] I. R. Mann,[3,4] N. P. Meredith,[5] J. B. Blake,[1] J. F. Fennell,[1] M. D. Looper,[1] D. K. Milling,[3,4] and R. R. Anderson[6]

Received 18 November 2002; revised 28 April 2003; accepted 7 May 2003; published 26 August 2003.

[1] We examine signatures of two types of waves that may be involved in the acceleration of energetic electrons in Earth's outer radiation belts. We have compiled a database of ULF wave power from SAMNET and IMAGE ground magnetometer stations for 1987–2001. Long-duration, comprehensive, in situ VLF/ELF chorus wave observations are not available, so we infer chorus wave activity from low-altitude SAMPEX observations of MeV electron microbursts for 1996–2001 since microbursts are thought to be caused by interactions between chorus and trapped electrons. We compare the ULF and microburst observations to in situ trapped electrons observed by high-altitude satellites from 1989–2001. We find that electron acceleration at low L shells is closely associated with both ULF activity and MeV microbursts and thereby probably also with chorus activity. Electron flux enhancements across the outer radiation belt are, in general, related to both ULF and VLF/ELF activity. However, we suggest that electron flux peaks observed at $L \sim 4.5$ are likely caused by VLF/ELF wave acceleration, while ULF activity probably produces the dominant electron acceleration at geosynchronous orbit and beyond. *INDEX TERMS:* 2720 Magnetospheric Physics: Energetic particles, trapped; 2716 Magnetospheric Physics: Energetic particles, precipitating; 2730 Magnetospheric Physics: Magnetosphere—inner; 2740 Magnetospheric Physics: Magnetospheric configuration and dynamics; *KEYWORDS:* magnetosphere, magnetic storms, radiation belts, relativistic electrons, ULF waves, VLF waves, microbursts, energetic electrons

Citation: O'Brien, T. P., K. R. Lorentzen, I. R. Mann, N. P. Meredith, J. B. Blake, J. F. Fennell, M. D. Looper, D. K. Milling, and R. R. Anderson, Energization of relativistic electrons in the presence of ULF power and MeV microbursts: Evidence for dual ULF and VLF acceleration, *J. Geophys. Res.*, *108*(A8), 1329, doi:10.1029/2002JA009784, 2003.

1. Introduction

[2] Author's note: During the revision of this manuscript, our dear friend and colleague Kirsten Lorentzen passed away suddenly. We hope that in its final form this manuscript maintains the high standards she exemplified.

[3] Following some magnetic storms, energetic (MeV) electron flux becomes enhanced in Earth's outer radiation belt. The outer radiation belt is a natural environment where physical processes occur that can neither easily be simulated nor synthesized in the laboratory. Many processes have been suggested that appear to be capable, if not culpable, of accelerating electrons to MeV energies from a lower energy source population. We present here a combination of a variety of observations into a superposed epoch comparison of magnetic storms that result in high MeV electron flux ("events") with storms that result in low MeV electron flux ("nonevents").

[4] We begin with a description of the phenomenology of MeV electrons in the outer radiation belts, followed by a brief review of proposed acceleration mechanisms. Then we proceed with our data analysis, which will include ground observations of ULF waves, low-altitude observations of bursty MeV electron precipitation (microbursts), which we use as a proxy for VLF waves, and fluxes of trapped electrons themselves. Finally, we suggest that a dual electron acceleration process, which includes both local acceleration by VLF waves and diffusive energization and transport by ULF waves, is consistent with our observations and analysis.

1.1. Energetic Electron Phenomenology

[5] Energetic electron acceleration appears to be associated with magnetic activity combined with high solar wind velocity. The role of magnetic activity has been assumed since the 1960s, when *Williams* [1966] established that the

[1]Space Science Department, The Aerospace Corporation, El Segundo, California, USA.
[2]Deceased 28 December 2002.
[3]Department of Physics, University of York, York, UK.
[4]Now at Department of Physics, University of Alberta, Edmonton, Alberta, Canada.
[5]Mullard Space Science Laboratory, University College London, Dorking, Surrey, UK.
[6]Department of Physics and Astronomy, University of Iowa, Iowa City, Iowa, USA.

0148-0227/03/2002JA009784$09.00

radiation belts exhibited periodicities consistent with the solar rotation period. Later, the solar connection was refined when *Paulikas and Blake* [1979] established that solar wind velocity was well correlated with trapped energetic electron fluxes. On the basis of further studies of upstream conditions, which showed that southward interplanetary magnetic field (IMF), in addition to high solar wind velocity, enhanced trapped electron radiation, it is likely that at least some level of magnetic activity is required for electron acceleration [*Baker*, 1996; *Baker et al.*, 1997; *Obara et al.*, 1998; *Iles et al.*, 2002]. It is also clear that magnetic storms greatly alter the electron belts, whether to empty them or to refill them [*Friedel et al.*, 2002; *Reeves et al.*, 2003].

[6] Whatever the response of the radiation belts to a magnetic storm, all L shells appear to respond similarly, on long enough timescales [*Kanekal et al.*, 2001]. Fast loss into the magnetopause and atmosphere can alter the radiation belts on timescales of a few hours. Slower loss processes, such as weak pitch angle scattering or coulomb drag, which is slow at high altitude, governs the decay of the radiation belts over days to weeks, should the magnetosphere remain quiet for such long intervals. Electron acceleration, however, almost always occurs on a relatively short timescale, in association with at least a small amount of magnetic activity. Typical timescales are $\sim$2 days between the onset of magnetic activity or high solar wind velocity and the peak in the radiation belt fluxes for fluxes of 3 MeV electrons at geosynchronous orbit [*Paulikas and Blake*, 1979; *Baker et al.*, 1990], or 1–2 days for low-altitude fluxes of >400 keV electrons over a range of L values [*Baker et al.*, 1994].

[7] In addition to the timescale constraint for electron acceleration, considerable information about the acceleration process can be inferred from the spatial (L) structure of the trapped MeV electrons. Satellites whose orbits cut through the radiation belts, crossing L shells, tend to observe a peak in flux versus L at a given energy. This peak resides in the vicinity of $L \sim 3-5$ for MeV electrons. The location of this peak, at least for storm-generated relativistic electrons, appears to be controlled by the minimum *Dst* of the storm [*Tverskaya*, 1986, 1996; *Iles et al.*, 2002; *Tverskaya et al.*, 2002]. *Tverskaya et al.* [2002] gives

$$L_{\max} \sim 12.9/|\min Dst|^{1/4} \quad (1)$$

as the relationship between the electron flux peak and minimum *Dst*.

[8] A more elusive, and potentially more valuable, observation is that of phase space density structure in L. The calculation of phase space density requires an accurate magnetic field model, which, to date, does not exist for disturbed time periods. *Selesnick and Blake* [2000] used a variety of magnetic field models to determine whether there was evidence for meaningful L structure in electron phase space densities derived from Polar observations. They concluded that there was no evidence for a peak interior to $L \sim 4$, but that existing field models disagree at higher L. *Green* [2002] attempted to resolve the magnetic field model problem with a sensitivity analysis and found what appeared to be a robust peak in electron phase-space density at $L \sim 5$ for several storms in 1998 observed by Polar. There is relatively good evidence that phase space density is typically higher at geosynchronous orbit than at $L \sim 4.5$ [*Hilmer et al.*, 2000; *McAdams et al.*, 2001]. However, whether any important structure exists between these two altitudes remains in dispute. It is also unclear what equation (1) tells us about phase-space density.

[9] Finally, it is appropriate to include a brief discussion of lower energy electrons. Geosynchronous satellites routinely observe dispersionless injections of energetic electrons associated with substorms [*Li et al.*, 1998]. The injected electrons bear typical energies of 10s to 100s of keV. *Kim et al.* [2000] showed that it is at least possible that some small fraction of the injected electrons achieve MeV energies, and *Ingraham et al.* [2001] provided an event study that suggests substorms can indeed inject substantial quantities of MeV electrons through geosynchronous orbit.

[10] At still lower energies, the plasmasphere is full of "cold" electrons, with typical energies around 1 eV. These electrons nominally extend from low altitude to about $L \sim 4.5$, and they drift around Earth once per day (corotation). The plasmasphere is believed to fill over several days from the ionosphere, so that the outer edge of the plasmasphere, the plasmapause, can extend well beyond $L \sim 4.5$ during quiet times. However, as activity increases, the outer layers of the plasmasphere are stripped off, bringing the plasmapause to as low as $L \sim 2$ [see, for example, *Carpenter and Anderson*, 1992; *Moldwin et al.*, 2002]. Recent work by *O'Brien and Moldwin* [2003] shows that the location of the plasmapause L_{pp} (without regard to local time) can be modeled as a function of the minimum *Dst* observed over the past 24 hours:

$$L_{pp} \sim 6.3 - 1.57 \log_{10} |Dst|. \quad (2)$$

[11] Interestingly, the L_{pp} model described by *O'Brien and Moldwin* [2003] in equation (2) resembles the $L_{\max}$ model described by *Tverskaya et al.* [2002] in equation (1). Whereas different functional forms were chosen for the two models, over the range of minimum *Dst* commonly expressed by the magnetosphere, the two functions are actually quite similar. Figure 1 shows that $L_{\max} \sim 1.3\ L_{pp}$ for *Dst* ranging from about -40 to -500 nT. Also included in the figure are several flux peaks in >1 MeV electrons determined from SAMPEX (Solar, Anomalous and Magnetospheric Particle Explorer) (for instrument description, see *Klecker et al.* [1993]) and in >1.5 MeV electrons determined from the HEO3 (1997–068) satellite (for instrument description, see *Blake et al.* [1997]). The uncertainty in the $L_{\max}$ determination is indicated by the vertical lines connecting multiple peaks (measured by a single spacecraft on successive passes through the radiation belts). Within the scatter of the data, the flux increases fit both the $L_{\max}$ curve from *Tverskaya et al.* [2002] and the $1.3\ L_{pp}$ curve, after *O'Brien and Moldwin* [2002]. We note that the factor 1.3 may depend on energy. The correspondence of the $L_{\max}$ and L_{pp} curves suggests that the relationship attributed to currents by *Tverskaya et al.* [2002] may be more closely related to the plasmapause. We will return to the implications of this relationship below.

1.2. Electron Acceleration Mechanisms

[12] *Friedel et al.* [2002] cite at least nine different mechanisms for generating relativistic electrons in the outer radiation belts, of which only a subset will be treated here.

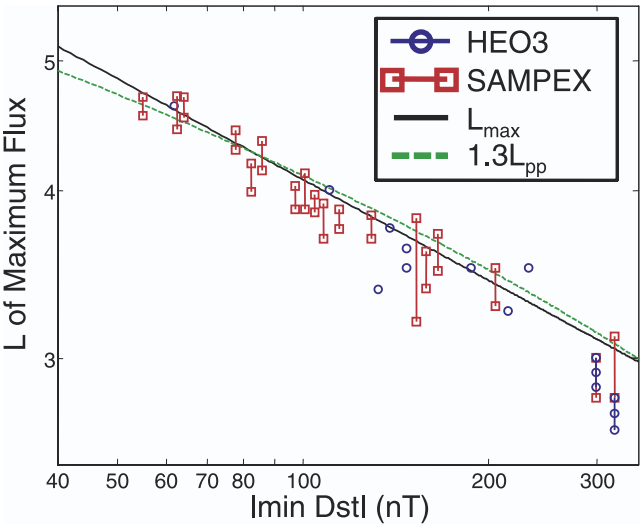

Figure 1. The location of the peak electron flux in the >1.5 MeV electron channel on the HEO3 spacecraft and >1 MeV electron channel on the SAMPEX spacecraft as a function of minimum *Dst*. Also plotted are the function L_{max} from *Tverskaya et al.* [2002] and a scaled plasmapause model L_{pp} from *O'Brien and Moldwin* [2002].

In all cases, it is common to assume a seed population of ~100 keV electrons provided by substorms and convection. We will break the acceleration models into categories based on which waves are involved: ULF models, VLF models, and hybrid models.

[13] *Falthammar* [1968] described what has come to be known as "simple" radial diffusion. In this model electromagnetic perturbations with spectral power at the frequency of an electron's drift orbit can cause stochastic diffusion in the drift invariant (L) while preserving the cyclotron and bounce invariants of the electron's motion. As the electron moves to lower L and stronger magnetic field, it gains energy. The frequency range of interest for energetic electrons in the inner magnetosphere is roughly 1–10 mHz, part of the ULF band. Diffusive transport will produce a net flow of electrons from regions of high phase-space density to lower density. If, as noted above, the phase space density is higher at geosynchronous than at $L \sim 4.5$, then radial diffusion will carry electrons inward, predominantly. Simple radial diffusion is less effective off the equator and at lower L, and does not result in any pitch angle scattering (which violates the cyclotron and bounce invariants) [*Falthammar*, 1968; *Schulz and Lanzerotti*, 1974, pp. 89–90]. Therefore simple radial diffusion should produce a pitch angle distribution that is peaked for equatorially mirroring particles, and should be progressively less effective at lower L (e.g., proportional to L^6 or higher order). Additionally, without breaking the cyclotron invariant, >4 MeV electrons arriving at $L \sim 4.5$ would have to have initial energies of >1 MeV in a ~30 nT field in the source region at $L \sim 10$. Recently, a form of enhanced radial diffusion has been suggested in which the asymmetry of the magnetic field in the inner magnetosphere allows more wave modes to act, with greater effect, on the energetic electrons [*Hudson et al.*, 1999, 2000, 2001; *Elkington et al.*, 1999, 2003]. This mechanism has been shown to be successful in modeling several energetic electron enhancements. However, because of the strong L dependence of radial diffusion and stronger losses at lower L, doubts have been expressed as to whether it can be effective far inside of geosynchronous orbit (R. M. Thorne et al., manuscript in preparation, 2003). Also, some case studies have found that radial diffusion is unable to reproduce the observed behavior of the radiation belts during selected storms [*Brautigam and Albert*, 2000; *Miyoshi et al.*, 2003]. The questions then that cast doubt on radial diffusion models are: What is the source population, and can radial diffusion transport particles efficiently enough to low L?

[14] Another acceleration model that relies completely on ULF waves is the global recirculation model. *Fujimoto and Nishida* [1990] suggested that ULF waves give rise not only to radial transport near the magnetic equator, but also to fast, elastic radial scattering at low altitudes. In this scenario electrons are continually scattered to higher L at low altitudes to be brought in again, and energized again, by radial diffusion near the equatorial plane. Considerable doubt persists as to whether the low-altitude phase of this recirculation process actually occurs. If it does occur, global recirculation should produce electron pitch angle distributions with an apparent source of particles near the loss cone (field aligned).

[15] *Summers and Ma* [2000b] suggested that ULF waves could accelerate electrons by violating the adiabatic invariant associated with electron cyclotron motion. When the bounce motion of an electron carries it through a ULF wave, the ULF wave can appear, by Doppler shift, to have a frequency resonant with the cyclotron frequency of the electron. This resonant interaction allows an electron and ULF wave to exchange energy, violating all three of the electron's adiabatic invariants, and possibly energizing the electron while damping the wave. Aside from the original analysis by *Summers and Ma* [2000b], this mechanism has not received further treatment in the literature.

[16] Considerable theoretical research has been done on potential acceleration (or heating) of energetic electrons by VLF/ELF waves [*Horne and Thorne*, 1998; *Summers et al.*, 1998, 2001; *Roth et al.*, 1999; *Summers and Ma*, 2000a]. Waves with frequencies that can be Doppler shifted to be near the electron gyrofrequency can readily interact with the cyclotron motion of trapped electrons. These waves come in many varieties: electromagnetic ion cyclotron waves (EMIC), whistler mode chorus, and auroral kilometric radiation (AKR), to name a few. In a comprehensive treatment, *Summers et al.* [1998] suggested that dusk-side EMIC waves at the plasmapause could isotropize energetic electrons, while dawn-side chorus energized and anisotropized the same electrons. This two-phase, longitudinal recirculation process would lead to nearly isotropic pitch angle distributions, with strong precipitation on the dusk side and slight anisotropy on the dawn side.

[17] Several recent studies have reported an association between relativistic electron flux enhancements and enhanced chorus amplitudes [*Meredith et al.*, 2002a; *Miyoshi et al.*, 2003; *Meredith et al.*, 2003]. Further evidence for electron acceleration to relativistic energies driven by whistler mode chorus has come from detailed studies of the 9 October 1990 geomagnetic storm. *Meredith et al.* [2002b] demonstrated that the observed spectral hardening

took place over a range of energies appropriate to the resonant energies associated with Doppler-shifted cyclotron resonance. *Horne et al.* [2003] observed flat-topped pitch angle distributions from $L \sim 4-6$ during the recovery phase of this storm, providing further evidence for chorus-driven acceleration. *Summers et al.* [2002] developed a model kinetic equation for the electron distribution and, using realistic wave and particle data from the CRRES spacecraft for this storm, were able to successfully reproduce the observed spectral hardening seen at $L \sim 4$.

[18] The electron distribution in velocity space is such that lower-band chorus, 10–50% of the electron gyrofrequency, can gain energy from lower energy (hundreds of keV) electrons near the loss cone while energizing MeV electrons closer to 90 degrees [*Meredith et al.*, 2002b; *Horne et al.*, 2003]. This local acceleration mechanism would be most effective near the plasmapause, and would not involve substantial radial transport. The energization is achieved diffusively in the presence of a phase-space gradient, producing net transport toward higher energy and 90 degree pitch angles along diffusion surfaces. The chorus interaction would be strongest near the plasmapause, where a local minimum in the ratio of the electron plasma to cyclotron frequencies coincides with strong lower-band chorus. Additionally, off-equatorial interactions between chorus and MeV electrons might produce microbursts [*Horne and Thorne*, 2003].

[19] Some authors have suggested hybrid acceleration mechanisms that involve both ULF and VLF waves playing complementary roles. A localized recirculation model has been suggested by *Boscher et al.* [2000]. In this model, radial diffusion transports particles inward at the equator and outward at higher latitudes, while plasmaspheric hiss provides pitch angle scattering inside the plasmapause. Near the plasmapause, electrons can locally recirculate many times, gaining energy with each cycle. Along these same lines, *Liu et al.* [1999] suggested a recirculation mechanism where radial diffusion by ULF waves and an unspecified pitch angle scattering mechanism (possibly whistler mode VLF waves) produced diffusion in energy space away from low energies. However, without specification of the crucial pitch angle scattering mechanism, this acceleration cannot yet be evaluated empirically.

[20] There are clearly a variety of electron acceleration mechanisms available, and nature tends to produce whatever is not forbidden. Nonetheless, some acceleration mechanisms are likely to be more important than others. In the following sections, we will provide observational evidence in an attempt to prioritize the available acceleration mechanisms, especially with regard to relative importance of ULF and VLF/ELF waves.

2. ULF Wave Observations

[21] Many recent observations have highlighted the association between ULF waves and energetic electrons, particularly at geosynchronous altitude. Consistent with the correlation between energetic electrons and high solar wind velocity, ULF waves can be generated by a Kelvin-Helmholtz shear flow instability across the magnetopause when magnetosheath (and therefore solar wind) velocity is sufficiently high [*Pu and Kivelson*, 1983; *Engebretson et al.*, 1998; *Mann et al.*, 1999; *Mathie and Mann*, 2000b, and references therein]. *Rostoker et al.* [1998] found that MeV electron fluxes at geosynchronous were well correlated with ULF wave power over a 90-day interval in 1994. *Baker et al.* [1998b] provided an event study in which ULF power appeared to be associated with the enhancement of MeV electron fluxes in the outer belt. *Baker et al.* [1998a] compared two storms and concluded that the electron accelerator involved ULF pulsations accelerating a seed population injected by substorms. Superposed epoch analyses have shown that magnetic storms resulting in high energetic electron fluxes tend to have sustained ULF power during the recovery phase [*Mathie and Mann*, 2000a; *O'Brien et al.*, 2001a; *Green and Kivelson*, 2001].

[22] We have analyzed ULF power (1–10 mHz) from the SAMNET (recording in magnetic H, D, and Z coordinates) and IMAGE (recording in geographic X, Y, and Z coordinates) magnetometer arrays [*Yeoman et al.*, 1990; *Viljanen and Hakkinen*, 1997] for 1987–2001. We have calculated the ULF power in all three magnetic components at several stations ranging in L from ~2.6 to ~6.9, given in Table 1. The time resolution of the data varies from 5–20 s over the history of the database. We measure ULF power in a 2-hour window centered on each hour of magnetic local time (MLT). We taper with a normalized Hanning window and apply a discrete Fourier transform. We then sum, for each component, the squared amplitude in the 1–10 mHz band. Our analysis only measures the spectral power in the specified frequency range. Because radial diffusion proceeds regardless of whether the wave power is narrowband (wave-like) or broadband (trend-like) [*Falthammar*, 1968; *Elkington et al.*, 2003], we have made no distinction in our data.

[23] We begin with a characterization of ULF power as a function of L and MLT. In Figure 2 we show ULF power conditioned by *Dst* and solar wind velocity (*Vsw*). (Interplanetary data are taken from the Omni database [*King and Papitashvili*, 1994].) At low solar wind velocity or weak *Dst*, ULF power is strongest on the night side at high L, with the peak moving to the day side at lower L. With higher solar wind velocity, the ULF power increases in general, while spreading away from midnight and to lower L. For active *Dst*, the enhancement is even stronger. Similar results for the dawn sector power have been found in previous studies [e.g., *Mathie and Mann*, 2000b, 2001].

[24] To determine the association between ULF power and energetic electrons, we perform a superposed epoch analysis following an algorithm similar to that of *O'Brien et al.* [2001a]. We have calculated a composite hourly noon electron flux from 1989–2001 for the 1.8–3.5 MeV electron channel on board Los Alamos National Laboratory geosynchronous satellites, using the statistical local time mapping algorithm described by *O'Brien et al.* [2001b]. We first identify magnetic storms in the interval 1989 through 2001 using *Dst*, requiring a *Dst* below −50 nT, with storm minima separated by at least 4 days. We then break these storms into two categories based on the composite noon electron flux at GEO ($L \sim 6.6$) averaged 48–72 hours after minimum *Dst*. Storms with average poststorm flux greater than 0.5 $cm^{-2}s^{-1}sr^{-1}keV^{-1}$ are classified as "events"; storms with average poststorm flux less than 0.5 $cm^{-2}s^{-1}sr^{-1}keV^{-1}$ are classified as "nonevents." The

Table 1. IMAGE and SAMNET Stations

Station	Magnetic Latitude, Degrees N	Magnetic Longitude, Degrees E	*L*
YOR	50.9	79.0	2.6
GML	54.9	78.2	3.1
FAR	60.8	78.1	4.3
PEL	63.6	105.4	5.1
MUO	64.7	105.7	5.6
KIL	65.8	104.5	6.1
KEV	66.3	109.7	6.3
SOR	67.3	106.7	6.9

threshold of 0.5 $cm^{-2}s^{-1}sr^{-1}keV^{-1}$ was chosen because it divides the storms into categories of approximately equal size. We have also considered categorization based on the ratio of poststorm flux to prestorm flux. The ratio method has two major problems that caused us to reject it: (1) it produces very dissimilar prestorm distributions of flux in the two categories, with "events" typically having low prestorm flux, and "nonevents" having high prestorm flux; and (2) the ratio method does not organize geophysical parameters, such as solar wind velocity, ULF power, and microburst frequency, as well as the poststorm flux threshold method. Essentially, our results rely on the fact that prestorm and poststorm fluxes are uncorrelated at geosynchronous orbit [*Reeves et al.*, 2003]. Our analysis implicitly assumes that nearly all electrons at geosynchronous are lost during the main phase of every storm, and the poststorm flux is determined entirely by the balance of acceleration and loss during the recovery phase.

[25] For each hour relative to the time of minimum *Dst* (epoch time zero), we obtain the distribution of each observable quantity in the two categories. For univariate time series (e.g., *Dst* or noon composite electron flux at GEO), we calculate the median and upper and lower quartiles of these distributions. For bivariate quantities, such as morning sector ULF wave power in the X or H component, we calculate the median power at each *L* (each station) by grouping the observations into four MLT sectors: predawn (00–06), morning (06–12), afternoon (12–18), and premidnight (18–24). Because each station can only be at one local time at any given time, we effectively have ULF measurements in each local time for one quarter of the storms. In Figure 3, we depict the evolution of X/H component ULF power and electron flux as a function of epoch time relative to minimum *Dst* for events and nonevents. We note that the *Dst* distributions are quite similar in the events and nonevents, with *Dst* recovering somewhat more slowly in events. This suggests that the magnetic field topology is likely (but by no means guaranteed) to be similar in the two sets of storms. For comparison with the geosynchronous data, we have also provided >1.5 MeV trapped fluxes at $L \sim 4.5$ from HEO1 (1994–026) (for instrument description, see *Blake et al.* [1997]). The electrons at $L \sim 4.5$ show a similar response to those at GEO during the recovery phase, indicating that the response is linked across *L* shells, as suggested by *Kanekal et al.* [2001]. We also notice that ULF power increases strongly with *L* in both categories of storms, regardless of local time sector, consistent with previous observations that ULF power increases with *L* [e.g., *Mathie and Mann*, 2001]. Additionally, in events and nonevents there is a burst of ULF power near minimum *Dst* in all sectors, with power stronger at higher *L* on the night side, consistent with Figure 2. Finally, we notice that the ULF power is much stronger in the events than in the nonevents, especially in the recovery phase. This reinforces what has been observed before [*Mathie and Mann*, 2000a; *O'Brien et al.*, 2001a; *Green and Kivelson*, 2001], suggesting that ULF waves play an important role in accelerating energetic electrons, particularly near geosynchronous orbit. In the next section we will examine whistler mode chorus, another wave band implicated in electron acceleration.

3. VLF/ELF Chorus Observations

[26] In a recent study, *Meredith et al.* [2001] sought to characterize the spatial dependence of chorus amplitudes as a function of substorm activity (as measured by *AE*) using CRRES in situ observations. They analyzed chorus amplitudes as a function of *AE*, band, magnetic latitude, *L*, and local time. They found that for $AE > 300$ nT, lower-band chorus (10–50% of the electron gyrofrequency) was excited beyond the nominal plasmapause and across the dawn side over a wide range of magnetic latitudes. (It should be noted that in some regions the lower-band chorus extends into the nominal ELF range, and therefore it is not strictly a VLF phenomenon, although it is often referred to as such in the literature). An example of the distribution of chorus waves is shown in Figure 4, which depicts the average equatorial lower-band chorus amplitude for $Kp \sim 4$–6 observed by CRRES. The equatorial region was defined as magnetic latitudes up to 15 degrees on either side of the magnetic equator. The CRRES spacecraft orbited for 15 months in 1990–1991, in a nearly equatorial geotransfer orbit with an

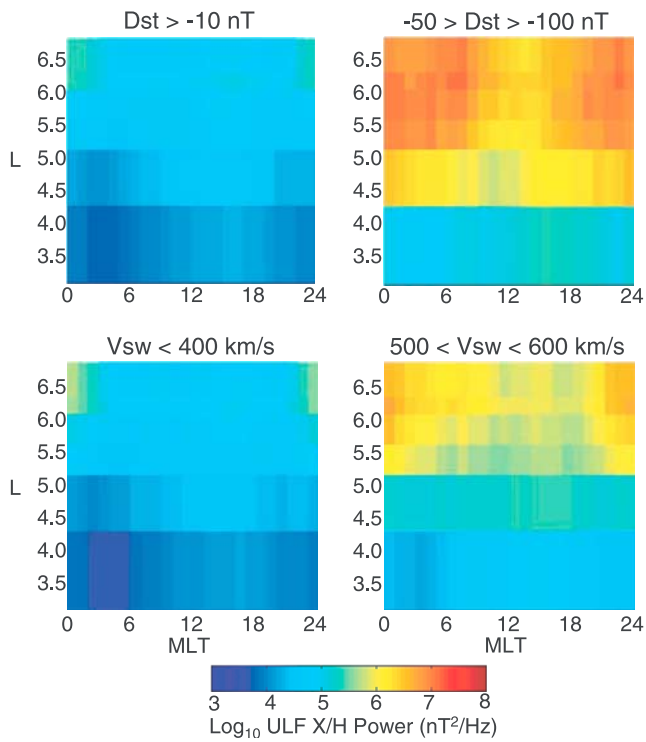

Figure 2. ULF X/H Power as a function of *L* and MLT for activity levels defined by *Dst* and *Vsw*.

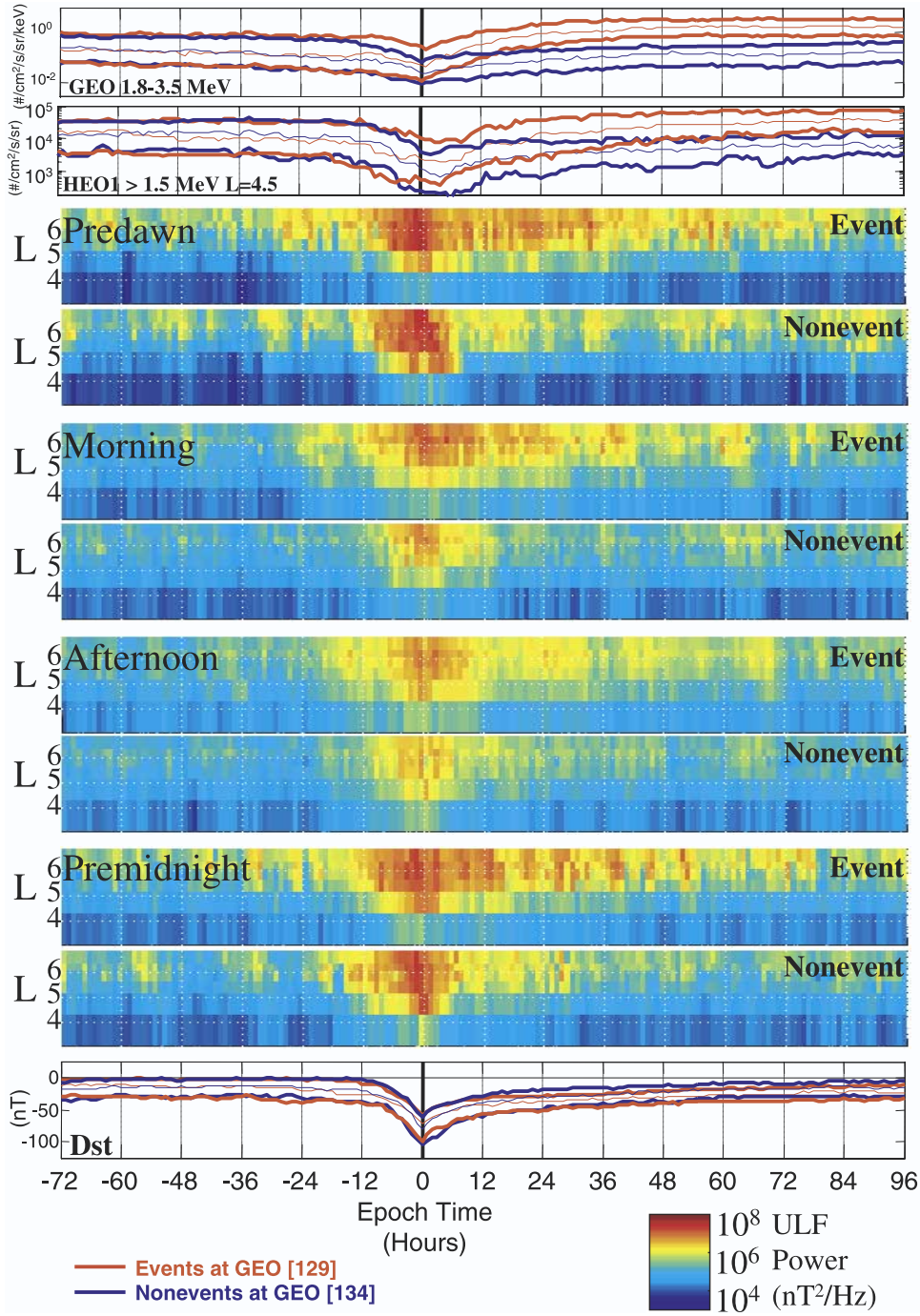

Figure 3. Superposed epoch depiction of electron flux, *Dst* and X/H ULF power for events and nonevents (see text). Thin red (blue) traces indicate the median at each epoch time for events (nonevents). Thick traces indicate the upper and lower quartiles. The color scale indicates median ULF power. Numbers in brackets indicate the number of storms in each category.

inclination of 18 degrees. The wave amplitudes in Figure 4 were derived from the Plasma Wave Experiment [*Anderson et al.*, 1992] from 939 CRRES orbits. For more information on the processing see *Meredith et al.* [2001]. It is clear in Figure 4, as was seen in the *Meredith et al.* [2001] study, that chorus activity is strongest on the dawn side, beyond the plasmapause. This is consistent with a model of chorus excited by substorm injection of 10–300 keV electrons, which are unstable to generation of chorus in the low-density region beyond the plasmapause.

4. Microburst Observations

[27] A number of researchers have reported ~1-s bursts of energetic electron precipitation (microbursts) in low-altitude observations from polar orbiting spacecraft [e.g.,

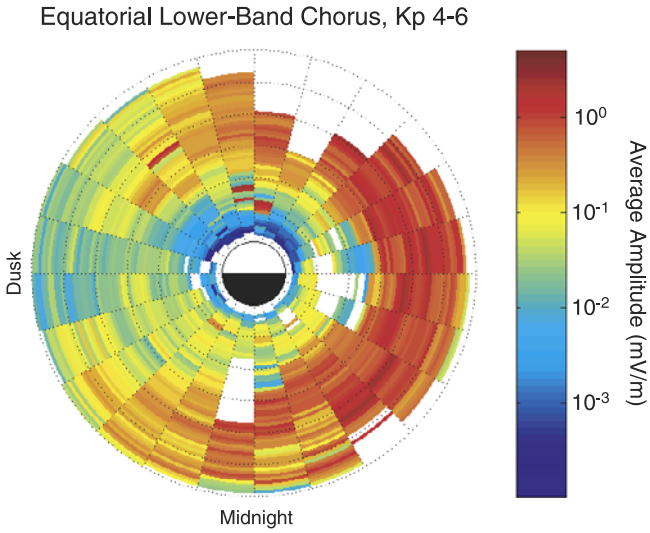

Figure 4. Average equatorial lower-band chorus amplitudes for *Kp* 4–6, observed by CRRES.

Brown and Stone, 1972; *Imhoff et al.*, 1992]. Recent research using data from SAMPEX has added extensively to this body of work [*Blake et al.*, 1996; *Nakamura et al.*, 1995, 2000; *Lyons et al.*, 1999; *Lorentzen et al.*, 2001a, 2001b]. We will first review briefly the results for subrelativistic microbursts followed by more recent results for relativistic microbursts.

[28] It is well established that subrelativistic microbursts are accompanied by chorus, although chorus can occur without generating microbursts [*Oliven and Gurnett*, 1968; *Parks*, 1978; *Rosenberg et al.*, 1981, 1990; *Roeder et al.*, 1985; *Torkar et al.*, 1987]. For electrons with energy of ~100 keV, cyclotron resonant interactions with chorus can readily occur near the magnetic equator, with resonant energy increasing off the equator. In fact, it is likely that 10–100 keV electrons are intimately associated with chorus. *Tsurutani and Smith* [1977] presented a picture of chorus generation in which substorms inject 10–100 keV electrons on the night side which subsequently convect around the dawn side. Because the magnetic field is not a perfect dipole and electrons with different pitch angles drift at different rates, substantial pitch angle anisotropy develops. When fluxes and anisotropy are high enough, the electron distribution becomes unstable to wave growth [*Kennel and Petschek*, 1966]. Whistler waves are generated near and below the local electron cyclotron frequency, which falls in the chorus band.

[29] Recent studies of relativistic microbursts have involved observations from the low-altitude, polar-orbiting SAMPEX mission. The Heavy Ion Large Telescope (HILT) instrument, which measures >1 MeV electrons, is described by *Klecker et al.* [1993], and the SAMPEX spacecraft as a whole is described by *Baker et al.* [1993]. *Blake et al.* [1996] showed that microbursts were often isotropic, but occurred over a range of L, indicating that they were not simply the result of a breakdown of adiabatic motion at the trapping boundary. By comparing conjugate passes, *Nakamura et al.* [1995] argued that microbursts were short-lived temporal structures rather than persistent spatial structures. Using a combination of event and statistical studies, *Nakamura et al.* [2000] showed an association between MeV microbursts and the dawnside plasmapause, suggesting that they were caused by whistler mode waves outside the plasmapause. On the basis of an enhancement of microbursts during storm intervals, they suggested that the microbursts were a side effect of electron acceleration. *Lorentzen et al.* [2001a] demonstrated that chorus was usually observed on the Polar spacecraft in conjunction with MeV microbursts on SAMPEX. From theoretical arguments, they demonstrated that a resonance between MeV electrons near the loss cone and chorus waves would require interaction at multiples of the gyrofrequency, interaction off the equator, or interaction in regions of depleted densities. However, it should be noted that their analysis applied only to electrons with pitch angles of 5 degrees; for the same plasma and wave conditions, the first-order cyclotron resonance is possible for electrons with pitch angles from 75–87 degrees at the equator. *Lorentzen et al.* [2001b] reinforced the association of microbursts with magnetic activity and the plasmapause while also calculating that the microburst precipitation was capable of emptying the prestorm radiation belt. Because microbursts are associated with magnetic activity and with chorus, they may be a side effect of the chorus heating mechanisms described above [*Horne and Thorne*, 1998; *Summers et al.*, 1998; *Summers and Ma*, 2000a; *Summers et al.*, 2001]. One scenario that satisfies the restrictions presented by *Lorentzen et al.* [2001a] has been suggested by *Horne and Thorne* [2003]. In their scenario, keV energy electrons near the equator generate chorus through a first-order cyclotron resonance, producing keV microbursts as a side effect. As the chorus wave packet propagates away from the equator, it could interact through the same first-order resonance with MeV electrons near the loss cone at higher latitude, scattering some of them into the loss cone and producing MeV microbursts. Combining this scenario with the earlier observations by *Lorentzen et al.* [2001a], we assume that microburst occurrence frequency can be used as a proxy for the interaction of chorus waves and energetic electrons.

[30] We have identified microbursts in SAMPEX >1 MeV electron measurements from 1996–2001 in 0.25L bins from $L \sim 2$–9. An L bin is considered to have microbursts if at any time during the SAMPEX pass through that L range a microburst is observed. Microbursts are defined as intervals when $(N_{100} - A_{500})/\sqrt{1 + A_{500}} > 10$, where the N_{100} is the number of counts in 100 ms and A_{500} is the centered running average of N_{100} over five 100 ms intervals (i.e., 0.5 s). We chose this definition because it compromises effectively between a linear measure of burstiness (N-A) and a logarithmic measure (N/A). We determined that a linear measure is oversensitive for large N and a logarithmic measure is oversensitive for small A. We confirmed that our definition agrees well with visual inspection for both high and low flux conditions.

[31] However, we must keep in mind some caveats regarding the microbursts as a proxy for chorus wave activity. The association between MeV microbursts and VLF/ELF chorus is not as well established as the relationship between keV microbursts and chorus; we have used the MeV microbursts because the keV microburst measurements from SAMPEX/HILT are not continuously available for multiple

years in a consistent instrument mode. Additionally, we cannot measure microbursts well when fluxes are very low because of poor counting statistics and the resulting bias inherent in our detection algorithm. This might lead to an artificial correlation between high trapped fluxes and high microburst occurrence frequency. Conversely, in the limit of strong pitch angle diffusion, the loss cone is full, and bursty enhanced precipitation signatures are masked by the strong precipitation. In the data we have collected for this study, the correlation between microburst frequency and trapped flux content observed by HEO is small (<0.01) for hourly averages, and so we continue to use MeV microbursts as a proxy for chorus wave activity in spite of the caveats. We note that using longer averages and time offsets results in stronger correlations, but such correlations are not evidence of a bias in the microburst detection algorithm.

[32] We must also consider some limitations to the wave-particle interaction between lower-band chorus and MeV electrons. *Lorentzen et al.* [2001a] showed that MeV electrons near the loss cone could only resonate with chorus off the equator, at multiples of the gyrofrequency, or in regions of depleted density. The strong lower-band chorus waves observed in the equatorial region on the dawn-side (see Figure 4) could interact with MeV electrons in each or all of these circumstances, especially as the waves propagate away from the equator. Indeed, inspection of the CRRES plasma wave data reveals that chorus waves are regularly observed at frequencies below 10% of the electron gyrofrequency at higher magnetic latitudes (15–30 degrees). We therefore feel justified in using the MeV microbursts as a proxy for the interaction between chorus and energetic electrons.

[33] The first step in our analysis of the microburst data is to extend the work of our predecessors by describing the distribution of MeV microbursts in MLT and *L*. *Lyons et al.* [1999] and *Lorentzen et al.* [2001a] showed that MeV microbursts were most common near midnight for low activity (*Kp* = 2) and in the prenoon sector for higher activity (*Kp* = 5–9). The midnight microbursts were qualitatively different from those in the prenoon sector, in that they were accompanied by fluctuations up to 30 s in duration [*Nakamura et al.*, 2000]. Additionally, the MeV prenoon microbursts moved to lower *L*, in association with the plasmapause and higher activity [*Nakamura et al.*, 2000; *Lorentzen et al.*, 2001a, 2001b]. *Lyons et al.* [1999] also included an analysis of >150 keV microbursts observed by SAMPEX in 1993; keV microbursts were found to be more common than the MeV variety, and occurred at somewhat higher *L* (although this may stem from a saturation bias at low *L* in the lower energy). It should be noted that the distribution of chorus depicted in Figure 4 agrees in *L* and local time with the distribution of MeV microbursts seen in previous studies [*Lyons et al.*, 1999; *Nakamura et al.*, 2000; *Lorentzen et al.*, 2001a], as expected if the two are causally connected. The *L* dependence exhibits a noteworthy exception: microburst frequency drops off more quickly with increasing *L* than does chorus amplitude. This drop-off may arise from the fact that the wave-particle interaction is strongest at the local minimum in the ratio of the electron plasma to cyclotron frequency just beyond the plasmapause, or it may simply be a result of the decreasing availability of trapped electrons at higher *L*. Figure 5 also shows that

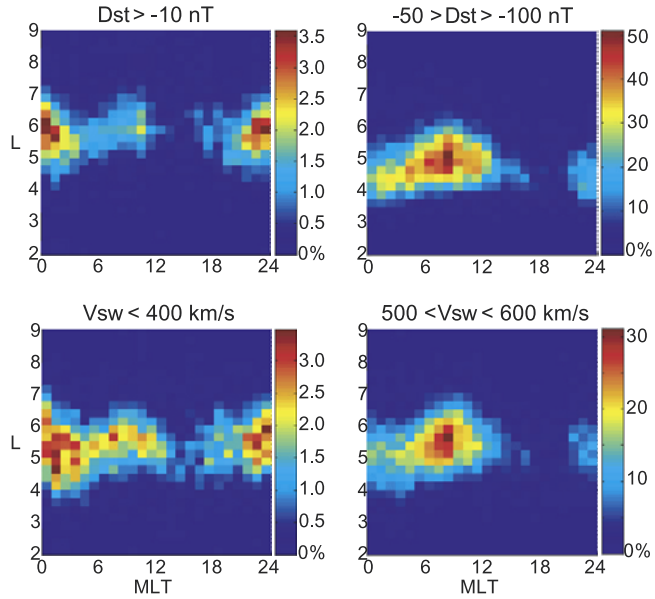

Figure 5. Microburst occurrence frequency as a function of *L* and MLT for activity levels defined by *Dst* and *Vsw*.

microburst location evolves similarly with *Dst* as described above for *Kp*: near midnight for weak activity, moving to the prenoon sector and lower *L* for increased activity. We emphasize that the color scales are different for each panel of Figure 5, allowing greater contrast within each figure. As observed for *Kp*, more activity in *Dst* tends to increase the microburst occurrence frequency. In the lower panels, Figure 5 shows that solar wind velocity *Vsw* between 500 and 600 km/s produces microbursts about 10 times more frequently than does *Vsw* < 400 km/s. However, *Vsw* does not, by itself, control the location of microbursts in *L*. There is substantial qualitative agreement for $L < 7$ between Figures 5 and 2, which describe microbursts and ULF power, respectively. The fact that microbursts become more common during high solar wind velocity indicates that they may explain part of the electron-*Vsw* relationship reported by *Paulikas and Blake* [1979], which has been previously attributed to ULF waves. In this scenario, higher solar wind velocity drives stronger magnetic activity [e.g., *McPherron*, 1998], which would enhance chorus as well as ULF wave activity.

[34] Next, we perform a superposed epoch analysis for the microbursts in much the same way as we did above for ULF waves. We use the same definition of events and nonevents; however, because our microburst data set only covers 1996–2001, we have about one third as many storms and a partial representation of the solar cycle. Figure 6 shows how MeV microbursts vary in occurrence frequency as a function of *L* and storm phase for four local time sectors. SAMPEX covers two local time sectors on any given orbit, so that the grouping into four local times halves the effective sample sizes. In the predawn and morning sectors both events and nonevents show an enhancement in microburst frequency around the time of minimum *Dst* over $L \sim 4$–5.5. In the events, this activity continues to be strong while rising to slightly higher *L* during the recovery phase.

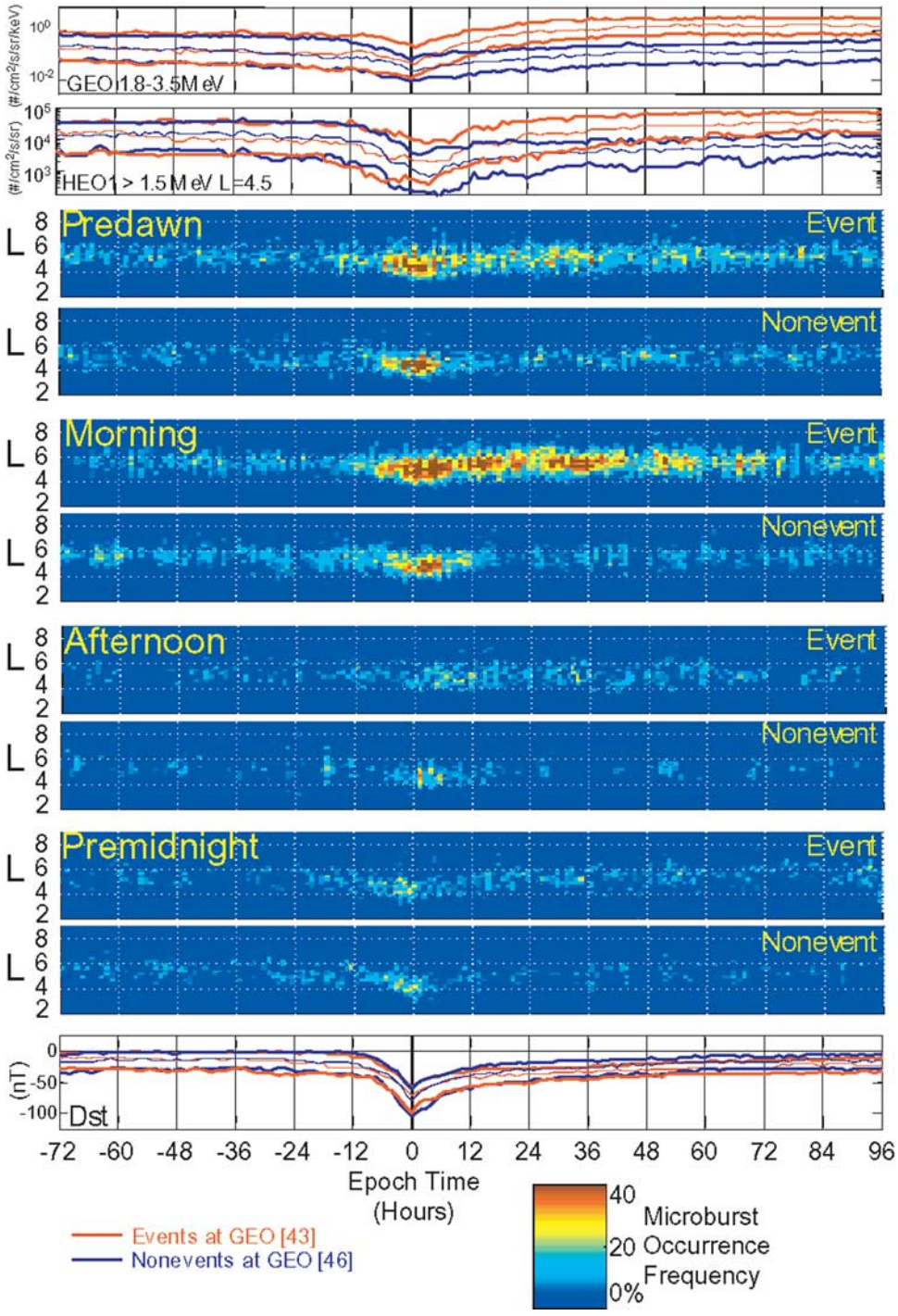

Figure 6. Superposed epoch depiction of electron flux, *Dst* and MeV microburst frequency for events and nonevents (see text). Red (blue) traces indicate median and upper and lower quartiles for events (nonevents). The color scale indicates microburst frequency. Numbers in brackets indicate the number of storms in each category.

Microbursts in the region of $L \sim 4.5-6$ remain active in the morning sector for several days following minimum *Dst*. As noted above, during this same interval the events at GEO coincide with considerably higher >1.5 MeV electron fluxes at $L \sim 4.5$ than the nonevents at GEO. Therefore it is clear that microbursts are associated with rising fluxes during the recovery phase and are not merely a side effect of high flux levels. It appears, then, that both microburst frequency and ULF wave power are enhanced in the recovery phase of magnetic storms that result in high MeV electron fluxes both at GEO and at $L \sim 4.5$.

5. ULF and Microburst Comparison

[35] If, as noted in the previous sections, electron events are characterized by more microbursts and stronger

ULF waves, some test needs to be done to determine whether either phenomenon alone or both in concert can be tied exclusively to electron acceleration. As a first step, we have designed what should be a simple test for this determination: we divide our magnetic storms into four categories based on the level of ULF power and the frequency of microbursts and compare the final MeV electron fluxes at several L shells. Approximately half of our storms exhibit ULF power in the X component averaged over all 4 local time sectors at Sorøyø (SOR) above 2.2×10^6 nT^2/Hz taken on the day (12–36 hours) after minimum *Dst*. Similarly, approximately half of our storms exhibit microburst probabilities above 2% averaged over all L. The microburst probability threshold appears low because it is averaged over all L and MLT, and it therefore includes the very low probability regions at $L \sim 2$ and $L \sim 9$ and near dusk, as well as the high probability region at $L \sim 4$–6 near dawn. These two thresholds allow us to divide our magnetic storms into four categories. In Figure 7 we depict the cumulative distribution of electron flux 72 hours after minimum *Dst* at three locations in each of the four categories. A cumulative distribution function describes the fraction of a sample that is less than the abscissa of the curve. At $L \sim 4.5$, poststorm HEO1 fluxes are nicely ordered as follows. Storms with neither strong ULF waves nor frequent microbursts have the lowest distribution of fluxes; storms with only ULF waves or microbursts have a somewhat higher distribution of fluxes; and storms with both strong ULF waves and frequent microbursts produce the highest poststorm fluxes at $L \sim 4.5$. At geosynchronous the storms exhibiting only ULF power or both ULF power and microbursts have similar distributions. The storms exhibiting only microbursts appear to result in mostly the same flux as the storms with ULF power, with a greater chance of a low final flux. Again, the storms with neither ULF power nor microbursts tend to result in lower fluxes than the other sets of storms. Finally, $L \sim 5.5$ gives an ordering between those at $L \sim 4.5$ and GEO. Taken together, these results suggest that near $L \sim 4.5$, microbursts and ULF power are equally associated with the final electron flux, whereas at geosynchronous orbit ULF wave power is more closely associated with electron acceleration.

[36] A note of caution is warranted in the interpretation of Figure 7: while we have attempted to use the most sensible criteria, different choices of the selection criteria allow the relative location of the distributions to change somewhat. Superposed epoch analyses have shown that the ULF power too close to minimum *Dst* is not correlated with the electron response [*Mathie and Mann*, 2000a; *O'Brien et al.*, 2001a; *Green and Kivelson*, 2001], and the same is true for microbursts (see, e.g., Figure 6). Similarly, if the selection criteria are moved too far after minimum *Dst*, the relevant activity may have died away after acceleration of the electrons. Therefore we have chosen for our analysis categories based on ULF power and microbursts 12–36 hours after minimum *Dst*. We have also performed the cumulative distribution analysis using only dawn ULF power. Such a change results in geosynchronous orbit, rather than $L \sim 4.5$, being the location at which the storms with only frequent microbursts or only high ULF power

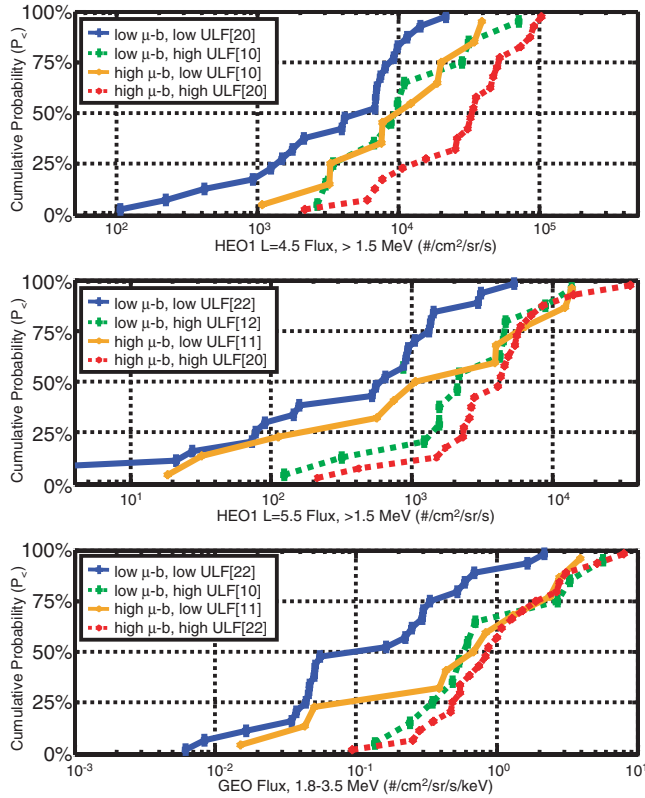

Figure 7. Cumulative distributions of electron flux 72 hours after minimum *Dst* for four categories based on high-latitude ULF power and microburst frequency. Fluxes at $L \sim 4.5$ and $L \sim 5.5$ are measured by HEO1, in the >1.5 MeV channel. Fluxes at GEO are composite noon LANL fluxes in a 1.8–3.5 MeV channel. The microburst (μ-b) frequency threshold is 2%, and the ULF power threshold is 2.2×10^6 nT^2/Hz. Numbers in brackets indicate the number of storms in each category for which data is available at a given L.

appear to have equivalent distributions of final flux. We have presented the results for an average over all sectors because we feel that, in a radial diffusion scenario, the electrons would respond to strong ULF power, regardless of its local time. We have also looked at the distribution of flux change for storms in each category, rather than the poststorm flux. While this slightly adjusts the distributions, it does not change the qualitative results. In all systems of categorization we have tried, the response of relativistic electrons tends to be more closely associated with ULF power at progressively higher L, and, conversely, it tends to be more closely associated with microbursts at progressively lower L.

6. Conclusion: Dual Acceleration

[37] The top portion of Figure 8 summarizes our findings of the location and intensity of microbursts and ULF wave power. The shading in the microburst region indicates the average occurrence frequency for $Kp \sim 4$–6, a distribution quite similar to the lower-band chorus distribution given in Figure 4. The waveforms indicate median ULF power in the X/H component for $Kp \sim 4$–6. The plasmapause location is

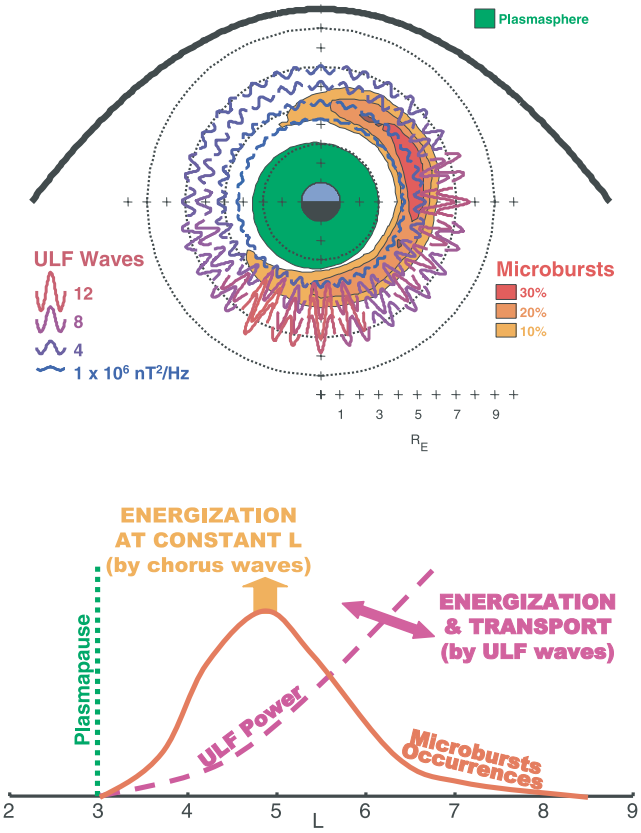

Figure 8. A composite sketch of electron acceleration. (top) The inner magnetosphere for $Kp \sim 4$–6. (bottom) A schematic of how and where ULF and VLF/ELF waves accelerate and transport electrons.

given by the *Kp*-based local-time-dependent model of *O'Brien and Moldwin* [2003] for $Kp_{\max} = 6$,

$$\phi = 2\pi(\mathrm{MLT}/24), \tag{3}$$

$$L_{\mathrm{pp}} \sim -0.39[1 - 0.34\cos(\phi - 2\pi \times 16.6/24)]Kp_{\max} + 5.6[1 + 0.12\cos(\phi - 2\pi \times 3/24)]. \tag{4}$$

[38] In large degrees, microburst frequency and ULF power exhibit surprising similarities. Both are strongest during the main phase of storms, both progress to lower L during stronger magnetic activity, both continue to be active during the recovery phase of events, and both appear to be more active during intervals of high solar wind velocity. The main distinctions between the two appears to be their distribution in L and MLT, and, possibly as a consequence, their association with poststorm flux at different L. We must, therefore combine the relatively small number of distinctions in the observations with theoretical arguments if we are to make any distinction between the roles of ULF and VLF/ELF waves in accelerating electrons to relativistic energies.

[39] We have observed that (1) microbursts of isotropic precipitation occur primarily on the dawn side, with greatest frequency near $L \sim 5$ and outside the plasmapause, (2) ULF wave power is stronger at higher L, and concentrated on the night and dawn sides, (3) strong ULF waves or frequent microbursts alone are associated with similar electron response at $L \sim 4.5$, while at higher L frequent microbursts alone are associated with a slightly weaker electron response than are strong ULF waves alone, and (4) strong ULF waves combined with frequent microbursts give a somewhat stronger electron response at all L shells. We are now faced with two competing explanations of the observations. First is the "loss only" explanation, in which microbursts are solely an indicator of loss. Second is the "side effect" explanation, in which microbursts are a side effect of electron energization by chorus waves.

[40] The "loss only" explanation argues that the MeV microbursts are purely a signature of loss, and that they play a role in shaping the L structure of the radiation belts only by carving away the electrons as they radially diffuse into the region just beyond the plasmapause. In this scenario, the chorus interaction described in the literature [e.g., *Horne and Thorne*, 1998; *Summers et al.*, 1998, 2001; *Summers and Ma*, 2000a; *Meredith et al.*, 2001, 2002a, 2002b; *Horne et al.*, 2003] would result primarily in loss, rather than acceleration. A comprehensive treatment of the loss versus acceleration efficiency of the chorus interaction has not been performed and is beyond the scope of this paper. However, the distribution of electrons in velocity space typically has gradients away from the loss cone and away from high energies [*Meredith et al.*, 2002b; *Horne et al.*, 2003]. In such cases, the diffusion curves for resonance with lower-band chorus waves allow particles with energies of hundreds of keV to give up energy to the waves while diffusing into the loss cone, and simultaneously particles at MeV energies gain energy from the waves while diffusing toward 90 degrees (see Figure 7 and *Meredith et al.* [2002b]). Also, the "loss only" argument would require radial diffusion to be strongly effective in the vicinity of the plasmapause, a requirement likely inconsistent with the drop-off in ULF wave power at lower L (as Vsw^L in the work of *Mathie and Mann* [2001]), and with the strong L dependence of radial diffusion (e.g., L^6 in the work of *Falthammar* [1968] or L^{11} in the work of *Elkington et al.* [2002]). Finally, the distribution of electron flux after microburst-only storms shown in Figure 7 is not consistent with their being only a loss process. We therefore conclude in favor of the "side effect" explanation, in which MeV microburst precipitation is interpreted as a side effect of electron acceleration by chorus.

[41] The bottom portion of Figure 8 is a smoothed, qualitative representation of the dawn profile of microburst occurrence frequency and ULF power (both in arbitrary linear scales). Arrows are drawn to indicate electron energization (vertical) and transport (horizontal). We suggest that in the vicinity of $L \sim 5$, or perhaps at $1.3L_{\mathrm{pp}}$ as indicated in Figure 1, chorus accelerates electrons without displacing them in L. Because the acceleration involves pitch angle scattering, microbursts are observed frequently in this VLF/ELF acceleration region. Closer to geosynchronous orbit, we suggest that ULF waves are more important, on average pushing electrons inward and energizing them.

[42] Since the microbursts appear to be caused by chorus interactions with trapped electrons, and such interactions are thought to accelerate some electrons that are not scattered

into the loss cone, we suggest that VLF/ELF chorus plays a significant role in accelerating the electrons, as proposed by, e.g., *Horne and Thorne* [1998]. We feel that there is also ample evidence that the radial diffusion and energization by ULF waves suggested, e.g., by *Elkington et al.* [2002] takes place in some form. Both ULF and VLF/ELF activity will contribute to electron acceleration throughout the outer zone, but ULF waves may play an increasingly dominant role at larger L, in particular beyond geosynchronous orbit. We make this distinction based on the fact that microburst activity decreases with L, while lower-band chorus amplitudes for $Kp \sim 4-6$ are relatively constant from the plasmapause to geosynchronous orbit and ULF amplitudes increase dramatically with L in the outer zone. At this time, we do not hypothesize any interaction between the ULF and chorus processes, which appear to overlap substantially in L, aside from noting that inward transport could help replenish those electrons that are lost to the atmosphere through the chorus wave interaction.

[43] It appears that during the recovery phase of electron events, chorus activity at $L \sim 5$ provides an inner magnetospheric source of MeV electrons, while the plasma sheet (and possibly substorms or other electron injections) provides a source of ~100 keV electrons at high L. Radial diffusion driven by ULF waves can redistribute both of these sources in L, filling the region between the plasma sheet and the plasmapause with trapped MeV electrons from both sources. Because radial diffusion is weak at low L, and ULF power is also weak at low L, the interior portion of the MeV electron belt probably arises mostly from VLF/ELF waves and the outer portion probably arises from inward transport from the plasma sheet. Since the interior portion of the belt includes a source, it is the likely location of a peak in phase-space density, which could produce a peak in flux at constant energy. The location of the peak in the radiation belts would be controlled by the VLF/ELF acceleration region, which appears to be excluded from the plasmasphere. Stronger magnetic storms have smaller plasmaspheres [e.g., *O'Brien and Moldwin*, 2003], and therefore deeper penetration of the radiation belts, in keeping with the observations of, e.g., *Tverskaya et al.* [2002].

[44] Our observations suggest that the VLF/ELF wave interaction occurs over a range of L, outside of the plasmapause. This suggests that coupled VLF-ULF acceleration local to the plasmapause, such as that advanced by *Boscher et al.* [2000], is probably not the dominant acceleration mechanism at low L. However, if the pitch angle-scattering role of plasmaspheric hiss in their model is achieved instead by whistler chorus, then the localized recirculation process may be active and important over the appropriate range of L. This scenario would have the ULF and VLF/ELF interactions linked, which is somewhat less parsimonious than the scenario described above, in which the wave interactions are independent. Additionally, based on Figure 7, it appears that either process alone can produce an electron response.

[45] We have several suggestions for further testing to falsify or validate the combined acceleration scenario we have suggested. First and foremost, attempts should be made to calculate correct phase-space density at a range of L values to determine whether there is evidence for a density peak in the vicinity of $L \sim 5$ in the early recovery phase. Such a peak would be consistent with a VLF/ELF accelerator. However, *Selesnick and Blake* [2000] showed that if the source population is variable, loss processes at high L can create a phase-space density peak after radial diffusion has brought new energetic electrons to the inner magnetosphere. Therefore it is necessary to observe carefully the temporal variations of the phase-space density. Appropriate efforts are already underway, including a study of several storms in 1998 using Polar observations which suggests that there is a phase-space density peak at $L \sim 5$ [*Green*, 2002]. Additionally, further empirical and theoretical study of the waves and wave-particle interactions that cause microbursts would be helpful, especially with regard to the relative efficiencies of acceleration and loss. Conjunction studies between low-altitude satellites like SAMPEX and higher altitude wave instruments, like Polar or Cluster, following *Lorentzen et al.* [2001a], would be very helpful. CRRES only covers about 15 months, and is therefore not sufficient for a comprehensive superposed epoch analysis of in situ waves; however, a study combining in situ ULF and VLF/ELF waves from CRRES, AMPTE, and SCATHA missions might cover enough storms for a superposed epoch analysis for electron events and nonevents, as shown here for ground-based ULF waves. Finally, global numerical simulations, like the Salammbo code [*Boscher et al.*, 2000], that can incorporate both VLF/ELF chorus and ULF wave-particle interactions could put the two mechanisms into a global perspective. Such simulations could be used to test the independence of the accelerators, as we have suggested, or the coupling of the accelerators suggested by *Boscher et al.* [2000]. Also, such models could be used to test whether the plasmapause location does, in fact, control the location of the peak intensity of the radiation belts.

[46] **Acknowledgments.** Work on this project at The Aerospace Corporation was supported by NASA grant NAG5-10972, University of Maryland contract Z667103, and U.S. Air Force contract F04701-93-C-0094. Partial support for the collaboration between Aerospace and York was obtained from U.K. P.P.A.R.C. grant PPA/G/O/2001/00021. SAMNET is a U.K. National Facility for solar-terrestrial physics operated and deployed by the University of York. The IMAGE data are collected as a Finnish-German-Norwegian-Polish-Russian-Swedish project. We acknowledge the following sources of additional data: the Kyoto World Data Center (WDC C-2) for geomagnetism and the observatories that produce *AE* and *Dst*, the National Geophysical Data Center and the observatories that produce *Kp*, OmniWeb and the numerous science teams that provided interplanetary data, and the Los Alamos energetic particles team. We acknowledge many helpful discussions with J. Green, V. Pilipenko, R. Thorne, and our colleagues at The Aerospace Corporation, at The University of York, and at Mullard Space Science Laboratory.

[47] Arthur Richmond thanks Scot Elkington and Mary K. Hudson for their assistance in evaluating this paper.

References

Anderson, R. R., D. A. Gurnett, and D. L. Odem, CRRES plasma wave experiment, *J. Spacecr. Rockets*, *29*, 570, 1992.

Baker, D. N., Solar wind-magnetosphere drivers of space weather, *J. Atmos. Sol. Terr. Phys.*, *58*, 1509, 1996.

Baker, D. N., R. L. McPherron, T. E. Cayton, and R. W. Klebesadel, Linear prediction filter analysis of relativistic electron properties at 6.6 R_E, *J. Geophys. Res.*, *95*, 15,133, 1990.

Baker, D. N., G. M. Mason, O. Figueroa, G. Colon, J. G. Watzin, and R. M. Aleman, An overview of the solar, anomalous and magnetospheric particle explorer (SAMPEX) mission, *IEEE Trans. Geosci. Remote Sens.*, *31*, 531, 1993.

Baker, D. N., J. B. Blake, L. B. Callis, J. R. Cummings, D. Hovestadt, S. Kanekal, B. Klecker, R. A. Mewaldt, and R. D. Zwickl, Relativistic electron acceleration and decay timescales in the inner and outer radiation belts: SAMPEX, *Geophys. Res. Lett.*, *21*, 409, 1994.

Baker, D. N., et al., Recurrent geomagnetic storms and relativistic electron enhancements in the outer magnetosphere: ISTP coordinate measurements, *J. Geophys. Res.*, *102*, 14,141, 1997.

Baker, D. N., T. I. Pulkkinen, X. Li, S. G. Kanekal, J. B. Blake, R. S. Selesnick, M. G. Henderson, G. D. Reeves, H. E. Spence, and G. Rostoker, Coronal mass ejections, magnetic clouds, and relativistic magnetospheric electron events: ISTP, *J. Geophys. Res.*, *103*, 17,279, 1998a.

Baker, D. N., et al., A strong CME-related magnetic cloud interaction with the Earth's magnetosphere: ISTP observation of rapid relativistic electron acceleration on May 15, 1997, *Geophys. Res. Lett.*, *25*, 2975, 1998b.

Blake, J. B., M. D. Looper, D. N. Baker, R. Nakamura, B. Klecker, and D. Hovestadt, New high temporal and spatial resolution measurements by SAMPEX of the precipitation of relativistic electrons, *Adv. Space Res.*, *18*, 171, 1996.

Blake, J. B., D. N. Baker, N. Turner, K. W. Ogilvie, and R. P. Lepping, Correlation of changes in the outer-zone relativistic-electron population with upstream solar wind and magnetic field measurements, *Geophys. Res. Lett.*, *24*, 927, 1997.

Boscher, D., S. Bourdarie, R. M. Thorne, and B. Abel, Influence of the wave characteristics on the electron radiation belt distribution, *Adv. Space. Res.*, *26*, 163, 2000.

Brautigam, D. H., and J. M. Albert, Radial diffusion analysis of outer radiation belt electrons during the October 9, 1990, magnetic storm, *J. Geophys. Res.*, *105*, 291, 1990.

Brown, J. W., and E. C. Stone, High-energy electron spikes at high latitudes, *J. Geophys. Res.*, *77*, 3384, 1972.

Carpenter, D. L., and R. R. Anderson, An ISEE/whistler model of equatorial electron density in the magnetosphere, *J. Geophys. Res.*, *97*, 1097–1108, 1992.

Elkington, S. R., M. K. Hudson, and A. A. Chan, Acceleration of relativistic electrons via drift-resonant interaction with toroidal-mode Pc-5 ULF oscillations, *Geophys. Res. Lett.*, *26*, 3273, 1999.

Elkington, S. R., M. K. Hudson, and A. A. Chan, Resonant acceleration and diffusion of outer zone electrons in an asymmetric geomagnetic field, *J. Geophys. Res.*, *108*(A3), 1116, doi:10.1029/2001JA009202, 2003.

Engebretson, M., K.-H. Glassmeier, M. Stellmacher, W. J. Hughes, and H. Lühr, The dependence of high-latitude Pc5 wave power on solar wind velocity and on the phase of high-speed solar wind streams, *J. Geophys. Res.*, *103*, 26,271, 1998.

Falthammar, C.-G., Radial diffusion by violation of the third adiabatic invariant, in *Earth's Particles and Fields*, Reinhold, New York, p. 157, 1968.

Friedel, R. H. W., G. D. Reeves, and T. Obara, Relativistic electron dynamics in the inner magnetosphere—A review, *J. Atmos. Sol. Terr. Phys.*, *64*, 265, 2002.

Fujimoto, M., and A. Nishida, Energization and anisotropization of energetic electrons in the Earth's radiation belt by the recirculation process, *J. Geophys. Res.*, *95*, 4265, 1990.

Green, J. C., Testing relativistic electron acceleration mechanisms, Ph.D. thesis, Univ. of Calif., Los Angeles, Calif., 2002.

Green, J. C., and M. G. Kivelson, A tale of two theories: How the adiabatic response and ULF waves affect relativistic electrons, *J. Geophys. Res.*, *106*, 25,777, 2001.

Hilmer, R. V., G. P. Ginet, and T. E. Cayton, Enhancement of equatorial energetic electron fluxes near L = 4.2 as a result of high speed solar wind streams, *J. Geophys. Res.*, *105*, 23,311, 2000.

Horne, R. B., and R. M. Thorne, Potential waves for relativistic electron scattering and stochastic acceleration during magnetic storms, *Geophys. Res. Lett.*, *25*, 3011, 1998.

Horne, R. B., and R. M. Thorne, Relativistic electron acceleration and precipitation during resonant interactions with whistler-mode chorus, *Geophys. Res. Lett.*, *30*(10), 1527, doi:10.1029/2003GL016973, 2003.

Horne, R. B., N. P. Meredith, R. M. Thorne, D. Heynderickx, R. H. A. Iles, and R. R. Anderson, Evolution of energetic electron pitch angle distributions during storm time electron acceleration to megaelectronvolt energies, *J. Geophys. Res.*, *108*(A1), 1016, doi:10.1029/2001JA009165, 2003.

Hudson, M. K., S. R. Elkington, J. G. Lyon, C. C. Goodrich, and T. J. Rosenberg, Simulation of radiation belt dynamics driven by solar wind variations, in *Sun-Earth Plasma Connections*, *Geophys. Monogr. Ser.*, vol. 109, edited by J. L. Burch et al., p. 171, AGU, Washington, D. C., 1999.

Hudson, M. K., S. R. Elkington, J. G. Lyon, and C. C. Goodrich, Increase in relativistic electron flux in the inner magnetosphere: ULF wave mode structure, *Adv. Space Res.*, *25*, 2327, 2000.

Hudson, M. K., S. R. Elkington, J. G. Lyon, M. J. Wiltberger, and M. Lessard, Radiation belt electron acceleration by ULF wave drift resonance: Simulation of 1997 and 1998 storms, in *Space Weather*, *Geophys. Monogr. Ser.*, vol. 125, edited by P. Song, p. 289, AGU, Washington, D. C., 2001.

Iles, R. H. A., A. N. Fazakerley, A. D. Johnstone, N. P. Meredith, and P. Buhler, The relativistic electron response in the outer radiation belt during magnetic storms, *Ann. Geophys.*, *20*, 957, 2002.

Imhoff, W. L., H. D. Voss, J. Mobilia, D. W. Datlowe, E. E. Gaines, J. P. McGlennon, and U. S. Inan, Relativistic electron microbursts, *J. Geophys. Res.*, *87*, 13,829, 1992.

Ingraham, J. C., T. E. Cayton, R. D. Belian, R. A. Christensen, R. H. W. Friedel, M. M. Meier, G. D. Reeves, and M. Tuszewski, Substorm injection of relativistic electrons to geosynchronous orbit during the great magnetic storm of March 24, 1991, *J. Geophys. Res*, *106*, 25,759, 1991.

Kanekal, S. G., D. N. Baker, and J. B. Blake, Multisatellite measurements of relativistic electrons: Global coherence, *J. Geophys. Res.*, *106*, 29,721, 2001.

Kennel, C. F., and H. E. Petschek, Limit on stably trapped particle fluxes, *J. Geophys. Res.*, *71*, 1, 1966.

Kim, H.-J., A. A. Chan, R. A. Wolf, and J. Birn, Can substorms produce relativistic outer belt electrons?, *J. Geophys. Res.*, *105*, 7721, 2000.

King, J. H., and N. E. Papitashvili, Interplanetary medium data book, suppl. 5, 1988–1993, Natl. Space Sci. Data Cent., Greenbelt, Md., 1994.

Klecker, B., et al., HILT: A heavy ion large area proportional counter telescope for solar and anomalous cosmic rays, *IEEE Trans. Geosci. Remote Sens.*, *31*, 542, 1993.

Li, X., D. N. Baker, M. Temerin, G. D. Reeves, and R. D. Belian, Simulation of dispersionless injections and drift echoes of energetic electrons associated with substorms, *Geophys. Res. Lett*, *20*, 3763, 1998.

Liu, W. W., G. Rostoker, and D. N. Baker, Internal acceleration of relativistic electrons by large-amplitude ULF pulsations, *J. Geophys. Res.*, *104*, 17,391, 1999.

Lorentzen, K. R., J. B. Blake, U. S. Inan, and J. Bortnik, Observations of relativistic electron microbursts in association with VLF chorus, *J. Geophys. Res.*, *106*, 6017, 2001a.

Lorentzen, K. R., M. D. Looper, and J. B. Blake, Relativistic electron microbursts during the GEM storms, *Geophys. Res. Lett.*, *28*, 2573, 2001b.

Lyons, L. R., H. E. J. Koskinen, J. Blake, A. Egeland, M. Hirahara, M. Oieroset, P. E. Sandholt, and K. Shiokawa, Processes leading to plasma losses into the high-latitude atmosphere, *Space Sci. Rev.*, *88*, 85, 1999.

Mann, I. R., A. N. Wright, K. J. Mills, and V. M. Nakariakov, Excitation of magnetospheric waveguide modes by magnetosheath flows, *J. Geophys. Res.*, *104*, 333, 1999.

Mathie, R. A., and I. R. Mann, A correlation between extended intervals of ULF wave power and storm-time geosynchronous relativistic electron flux enhancements, *Geophys. Res. Lett.*, *27*, 3261, 2000a.

Mathie, R. A., and I. R. Mann, Observations of Pc5 field line resonance azimuthal phase speeds: A diagnostic of their excitation mechanism, *J. Geophys. Res.*, *105*, 10,713, 2000b.

Mathie, R. A., and I. R. Mann, On the solar wind control of Pc5 ULF pulsation power at mid-latitudes: Implications for MeV electron acceleration in the outer radiation belt J, *Geophys. Res.*, *106*, 29,783, 2001.

McAdams, K. L., G. D. Reeves, R. H. W. Friedel, and T. E. Cayton, Multisatellite comparisons of the radiation belt response to the GEM magnetic storms, *J. Geophys. Res.*, *106*, 10,869, 2001.

McPherron, R. L., Determination of linear filters for predicting Ap during January 1997, *Geophys. Res. Lett.*, *25*, 3035, 1998.

Meredith, N. P., R. B. Horne, and R. R. Anderson, Substorm dependence of chorus amplitudes: Implications for the acceleration of electrons to relativistic energies, *J. Geophys. Res.*, *106*, 13,165, 2001.

Meredith, N. P., R. B. Horne, R. H. A. Iles, R. M. Thorne, D. Heynderickx, and R. R. Anderson, Outer zone relativistic electron acceleration associated with substorm-enhanced whistler mode chorus, *J. Geophys. Res.*, *107*(A7), 1144, doi:10.1029/2001JA900146, 2002a.

Meredith, N. P., R. B. Horne, D. Summers, R. M. Thorne, R. H. A. Iles, D. Heynderickx, and R. R. Anderson, Evidence for acceleration of outer zone electrons to relativistic energies by whistler mode chorus, *Ann. Geophys.*, *20*, 967, 2002b.

Meredith, N. P., M. Cain, R. B. Horne, R. M. Thorne, D. Summers, and R. R. Anderson, Evidence for chorus-driven electron acceleration to relativistic energies from a survey of geomagnetically disturbed periods, *J. Geophys. Res.*, *108*(A6), 1248, doi:10.1029/2002JA009764, 2003.

Miyoshi, Y., A. Morioka, T. Obara, H. Misawa, T. Nagai, and Y. Kasahara, Rebuilding process of the outer radiation belt during the 3 November 1993 magnetic storm: NOAA and Exos-D observations, *J. Geophys. Res.*, *108*(A1), 1004, doi:10.1029/2001JA007542, 2003.

Moldwin, M. B., L. Downward, H. K. Rassoul, R. Amin, and R. R. Anderson, A new model of the location of the plasmapause: CRRES results, *J. Geophys. Res.*, *107*(A11), 1339, doi:10.1029/2001JA009211, 2002.

Nakamura, R., D. N. Baker, J. B. Blake, S. Kanekal, B. Klecker, and D. Hovestadt, Relativistic electron precipitation enhancements near the outer edge of the radiation belt, *Geophys. Res. Lett.*, *22*, 1129, 1995.

Nakamura, R., M. Isowa, Y. Kamide, D. N. Baker, J. B. Blake, and M. Looper, SAMPEX observations of precipitation bursts in the outer radiation belt, *J. Geophys. Res.*, *105*, 15,875, 2000.

Obara, T., T. Nagatsuma, and T. G. Onsager, Effects of the interplanetary magnetic field (IMF) on the rapid enhancement of relativistic electrons in the outer radiation belt during the storm recovery phase, in *Fourth International Conference on Substorms*, p. 215, Kluwer Acad., Norwell, Mass., 1998.

O'Brien, T. P., and M. B. Moldwin, Empirical plasmapause models from magnetic indices, *Geophys. Res. Lett.*, *30*(4), 1152, doi:10.1029/2002GL016007, 2003.

O'Brien, T. P., R. L. McPherron, D. Sornette, G. D. Reeves, R. Friedel, and H. Singer, Which magnetic storms produce relativistic electrons at geosynchronous orbit?, *J. Geophys. Res.*, *106*, 15,533, 2001a.

O'Brien, T. P., D. Sornette, and R. L. McPherron, Statistical asynchronous regression: Determining the relationship between two quantities that are not measured simultaneously, *J. Geophys. Res.*, *106*, 13,247, 2001b.

Oliven, M. N., and D. A. Gurnett, Microburst phenomena: 3. An association between microbursts and VLF chorus, *J. Geophys. Res.*, *73*, 2355, 1968.

Parks, G. K., Microburst precipitation phenomena, *J. Geomagn. Geoelectr.*, *30*, 327, 1978.

Paulikas, G. A., and J. B. Blake, Effects of the solar wind on magnetospheric dynamics: Energetic electrons at the synchronous orbit, in *Quantitative Modeling of Magnetospheric Processes*, *Geophys. Monogr. Ser.*, vol. 21, edited by W. P. Olson, p. 180, AGU, Washington, D. C., 1979.

Pu, Z. Y., and M. G. Kivelson, Kelvin-Helmholtz instability at the magnetopause: Solution for compressible plasmas, *J. Geophys. Res.*, *88*, 841, 1983.

Reeves, G. D., K. L. McAdams, R. H. W. Friedel, and T. P. O'Brien, Acceleration and loss of relativistic electrons during geomagnetic storms, *Geophys. Res. Lett.*, *30*(10), 1529, doi:10.1029/2002GL016513, 2003.

Roeder, J. L., J. R. Benbrook, E. A. Bering III, and W. R. Sheldon, X ray microbursts and VLF chorus, *J. Geophys. Res.*, *90*, 10,975, 1985.

Rosenberg, T. J., J. C. Siren, D. L. Matthews, K. Marthinsen, J. A. Holtet, A. Egeland, D. L. Carpenter, and R. A. Helliwell, Conjugacy of electron microbursts and VLF chorus, *J. Geophys. Res.*, *86*, 5819, 1981.

Rosenberg, T. J., R. Wei, D. L. Detrick, and U. S. Inan, Observations and modeling of wave-induced microburst electron precipitation, *J. Geophys. Res.*, *95*, 6467, 1990.

Rostoker, G., S. Skone, and D. N. Baker, On the origin of relativistic electrons in the magnetosphere associated with some geomagnetic storms, *Geophys. Res. Lett.*, *25*, 3701, 1998.

Roth, I., M. Temerin, and M. K. Hudson, Resonant enhancement of relativistic electron fluxes during geomagnetically active periods, *Ann. Geophys.*, *17*, 631, 1999.

Schulz, M., and L. J. Lanzerotti, *Physics and Chemistry in Space*, vol. 7, *Particle Diffusion in the Radiation Belts*, Springer-Verlag, New York, 1974.

Selesnick, R. S., and J. B. Blake, On the source location of radiation belt relativistic electrons, *J. Geophys. Res.*, *105*, 2607, 2000.

Summers, D., and C. Ma, A model for generating relativistic electrons in the Earth's inner magnetosphere based on gyroresonant wave-particle interactions, *J. Geophys. Res.*, *105*, 2625, 2000a.

Summers, D., and C. Ma, Rapid acceleration of electrons in the magnetosphere by fast-mode MHD waves, *J. Geophys. Res.*, *105*, 15,887, 2000b.

Summers, D., R. M. Thorne, and F. Xiao, Relativistic theory of wave-particle resonant diffusion with application to electron acceleration in the magnetosphere, *J. Geophys. Res.*, *103*, 20,487, 1998.

Summers, D., R. M. Thorne, and F. Xiao, Gyroresonant acceleration of electrons in the magnetosphere by superluminous electromagnetic waves, *J. Geophys. Res.*, *106*, 10,853, 2001.

Summers, D., C. Ma, N. P. Meredith, R. B. Horne, R. M. Thorne, D. Heynderickx, and R. R. Anderson, Model of the energization of outer-zone electrons by whistler-mode chorus during the October 9, 1990 geomagnetic storm, *Geophys. Res. Lett.*, *29*(24), 2174, doi:10.1029/2002/GL016039, 2002.

Torkar, K. M., et al., A study of the interaction of VLF waves with equatorial electrons and its relationship to auroral X-rays in the morning sector, *Planet. Space Sci.*, *35*, 1231, 1987.

Tsurutani, B. T., and E. J. Smith, Two types of magnetospheric ELF chorus and their substorm dependences, *J. Geophys. Res.*, *82*, 5112, 1977.

Tverskaya, L. V., On the boundary of electron injection into the magnetosphere, *Geomagn. Aeron.*, *26*, 864, 1986.

Tverskaya, L. V., The latitude position dependence of the relativistic electron maximum as a function of D_{st}, *Adv. Space Res.*, *18*, 135, 1996.

Tverskaya, L. V., N. N. Pavlov, J. B. Blake, R. S. Selesnick, and J. F. Fennell, Predicting the L-position of the storm-injected relativistic electron belt, *Adv. Space*, in press, 2002.

Viljanen, A., and L. Hakkinen, IMAGE magnetometer network, in *Satellite-Ground Based Coordination Sourcebook*, *ESA Publ. SP-1198*, Eur. Space Agency, Paris, 1997.

Williams, D. J., A 27-day periodicity in outer zone trapped electron intensities, *J. Geophys. Res.*, *71*, 1815, 1966.

Yeoman, T. K., D. K. Milling, and D. Orr, Pi2 pulsation patterns on the UK Sub-Auroral Magnetometer NETwork (SAMNET), *Planet. Space Sci.*, *38*, 589, 1990.

R. R. Anderson, Department of Physics and Astronomy, University of Iowa, Iowa City, IA 52242-1479, USA. (roger-r-anderson@uiowa.edu)

J. B. Blake, J. F. Fennell, M. D. Looper, and T. P. O'Brien, M2-260, PO Box 92957, Space Science Department, The Aerospace Corporation, El Segundo, CA 90009-2957, USA. (JBernard.Blake@aero.org; Joseph.F.Fennell@aero.org; Mark.D.Looper@aero.org; paul.obrien@aero.org)

I. R. Mann and D. K. Milling, Department of Physics, University of Alberta, Edmonton, Alberta T6G 2J1, Canada. (imann@space.ualberta.ca; dmilling@phys.ualberta.ca)

N. P. Meredith, Mullard Space Science Laboratory, University College London, Holmbury St. Mary, Dorking, Surrey RH5 6NT, UK. (npm@mssl.ucl.ac.uk)